

3D geometric morphometrics in veterinary science: applications, standardization, and future directions

T. Szara¹, N. Hadžimerović², C. Bakıcı³, B. Can Güzel⁴, O. Gündemir^{5,6}

¹Department of Morphological Sciences, Institute of Veterinary Medicine, Warsaw University of Life Sciences-SGGW, 02-776 Warsaw, Poland

²Department of Basic Sciences of Veterinary Medicine, Veterinary Faculty, University of Sarajevo, 71000 Sarajevo, Bosnia and Herzegovina

³Department of Anatomy, Faculty of Veterinary Medicine, Ankara University, 06110 Ankara, Turkey

⁴Department of Anatomy, Faculty of Veterinary Medicine, Siirt University, Siirt, Turkey

⁵Department of Anatomy, Faculty of Veterinary Medicine, Istanbul University-Cerrahpaşa, 34320 Istanbul, Turkey

⁶Osteoarchaeology Practice and Research Centre, Istanbul University-Cerrahpaşa, 34320 Istanbul, Turkey

Correspondence to: T. Szara, e-mail: tomasz_szara@sggw.edu.pl

Abstract

Three-dimensional geometric morphometric methods have emerged as a pivotal tool in veterinary anatomy, taxonomy, clinical research, and studies of morphological diversity. This article summarizes the key stages, applications, clinical potential, and recommendations for data standardization in 3D morphometrics. Datasets are typically acquired using radiological modalities, including computed tomography (CT), magnetic resonance imaging (MRI), and 3D surface scanning, each offering specific advantages and constraints contingent on the research context. Standardized landmark sets are essential in 3D morphometric studies to ensure reproducibility and comparability of results across independent investigations. Consistent use of reference landmarks enables repeatable analyses, but the number of landmarks directly influences the required sample size and statistical power. Consequently, a minimal yet balanced landmark configuration is critical. This article proposes a standardized, minimal landmark set for the skulls of horses, cattle, and sheep to enhance inter-study reproducibility and comparability. Landmark selection prioritizes anatomically distinct points to avoid excessive landmarking, which may complicate analyses or compromise interpretability. Applications of 3D morphometric methods include orthopedic surgical planning, biomechanical modeling, and assessment of congenital anomalies, providing enhanced precision in diagnostics and research. In conclusion, 3D geometric morphometric methods represent a robust analytical framework in veterinary anatomy, morphology, and clinical research. Their significance is poised to grow through integration with automated landmarking, artificial intelligence-driven analyses, and international data-sharing networks, thereby advancing scientific inquiry in novel dimensions.

Keywords: biomechanical modeling, cranial landmarks, 3D geometric morphometrics, orthopedic surgical planning, veterinary anatomy



Introduction

Traditional morphological approaches, reliant on linear measurements, angular assessments, and qualitative descriptions, have historically dominated investigations of animal anatomy. However, these methods are limited in their ability to capture the three-dimensional complexity of anatomical structures and are susceptible to observer-dependent biases, which may compromise reproducibility (Zelditch et al. 2012). Recent advancements in three-dimensional (3D) digital technologies have catalyzed a paradigm shift in morphological research methodologies (Herzlinger et al. 2017, Hirst et al. 2018). High-resolution 3D scanning techniques, such as structured light and laser-based systems, alongside imaging modalities such as computed tomography (CT), magnetic resonance imaging (MRI), and photogrammetry, enable the generation of precise digital models for repeatable analyses of skeletal and soft tissue structures (Hennessy et al. 2005, Carballido-Gamio et al. 2008, Van der Niet et al. 2010).

Three-dimensional geometric morphometrics facilitates the statistical dissociation of shape and size, enabling the quantification of subtle morphological variations that are challenging to assess using conventional methods (Klingenberg 2016). This approach offers substantial advantages for comparative analyses across species, breeds, sexes, and age groups, as well as for investigating adaptive and functional traits (Hadžiomerović et al. 2023, Manuta et al. 2024, Korkmazcan et al. 2025). Studies of cranial morphology in domestic mammals, such as horses, cattle, and sheep, underscore the growing relevance of these technologies in veterinary anatomy, education, taxonomy, evolutionary biology, and archaeological research (Haruda et al. 2019, Bakici et al. 2025).

This review provides a comprehensive evaluation of the current state and potential of 3D analytical methods in animal morphology studies. It first examines key techniques for acquiring digital models, including 3D scanning, radiological imaging, and segmentation. Subsequently, it proposes a standardized set of cranial landmarks for horses, cattle, and sheep, illustrating their practical applications. Finally, it discusses prevalent statistical methods, such as Generalized Procrustes Analysis (GPA), Principal Component Analysis (PCA), and Canonical Variate Analysis (CVA), while exploring current and prospective applications of 3D morphometrics. This review aims to establish a methodological framework for researchers in veterinary anatomy, zoology, and taxonomy.

3D Model Acquisition

The acquisition of high-accuracy three-dimensional (3D) models constitutes a crucial step in geometric morphometric studies, as model resolution and fidelity significantly impact the reliability of subsequent statistical analyses. Three-dimensional models of animal anatomical structures are primarily generated using two complementary techniques: surface digitization (3D scanning) and radiological imaging with segmentation (Thali et al. 2003, Sood et al. 2021). Each method offers distinct advantages and limitations, depending on the specimen type and the study's specific objectives.

Surface digitization is widely used to rapidly and precisely capture the external morphology of rigid anatomical specimens, such as skeletal elements (Eravci Yalin et al. 2024, Pasicka et al. 2025). Structured light and laser-based 3D scanners offer sub-millimetre resolution, making them particularly suitable for structures such as skulls, long bones, and articular surfaces. However, this approach is limited to external morphology and cannot capture internal structures, such as trabecular bone, sinus cavities, or soft tissues (Bjørndal et al. 1999, Han et al. 2019, Tretiakow et al. 2021). Radiological imaging is thus essential for studies requiring internal anatomical details.

Computed tomography (CT) and magnetic resonance imaging (MRI) enable comprehensive 3D visualization of both hard and soft tissues, providing insights into internal structures, including intracranial cavities, trabecular bone, and organ morphology (İşbilir and Güzel 2023, Atli et al. 2025). However, CT data often exhibit lower spatial resolution compared to high-quality laser or structured light scanners, and the large datasets generated can pose computational challenges during post-processing. Additionally, the use of CT and MRI in studies involving live animals raises ethical concerns, particularly regarding radiation exposure and regulatory constraints. These concerns align with the 3R principles (Replacement, Reduction, Refinement): replacing existing models or using non-invasive alternatives where possible, reducing the number of animals imaged, and refining protocols to minimize exposure and distress. For osteological material (e.g., prepared skeletons), no such ethical issues apply, as imaging is non-invasive and involves no live subjects. In contrast, live animal imaging must adhere to regulatory frameworks, such as the ARRIVE 2.0 guidelines for transparent reporting of animal research (Percie et al. 2020).

Radiological image data are typically processed using 3D Slicer, Mimics, or Amira software to generate 3D models via segmentation (Fedorov et al. 2012, Haverkamp et al. 2019, Ahmed et al. 2023). Segmenta-

tion can be manual, semi-automatic, or fully automatic; however, manual refinement is often necessary for complex structures. The resulting 3D models are generally exported in STL, PLY, or OBJ formats for morphometric analyses.

The resolution of 3D models is primarily determined by the imaging device and acquisition parameters. While surface scanners generally offer superior geometric fidelity, CT and MRI provide critical insights into tissue differentiation and internal morphology. Therefore, the choice of method should align with the study's objectives. Prior to analysis, 3D models are often subjected to mesh decimation and data optimization to improve computational efficiency while preserving anatomical accuracy. Recommended quality-control indicators for reproducible model preparation include assessing surface smoothness after decimation, angular deviation, and curvature distribution.

Landmark selection and sample size considerations

This review proposes a minimal, simplified set of cranial landmarks for horses (Fig. 1, Table 1), cattle (Fig. 2, Table 2), and sheep (Fig. 3, Table 3) to facilitate three-dimensional (3D) geometric morphometric analyses. Minimizing the number of landmarks is critical for multivariate statistical methods, such as Principal Component Analysis (PCA), as an increased number of landmarks escalates dimensionality and degrees of freedom, thereby complicating analyses. The number of coordinates per specimen is determined as the product of the number of landmarks (L) and dimensionality (D). For instance, 36 landmarks in 3D yield 108 variables per individual ($36L \times 3D$). Although Generalized Procrustes Analysis (GPA) mitigates the effects of size (scale), position (translation), and orientation (rotation), thereby reducing degrees of freedom, the resulting data space remains high-dimensional, necessitating a sufficiently large sample size to ensure robust statistical outcomes. Generally, when employing 36 landmarks in 3D analysis (108 variables per specimen), the sample size (N) should exceed the total number of variables ($L \times D$) to ensure reliable multivariate analyses and prevent overfitting (Bookstein 1991, Zelditch et al. 2012).

The literature underscores that, for robust multivariate analyses, the sample size (N) must exceed the total dimensionality of the data, calculated as the product of the number of landmarks (L) and dimensionality (D) (Bookstein 1991, Zelditch et al. 2012). Small sample sizes can introduce significant biases, particularly in estimating variance and mean shape (Cardini

and Elton 2007, Cardini et al. 2015). Consequently, employing a minimal landmark set streamlines data processing, maintains a manageable sample size requirement, and ensures statistical reliability.

The minimal cranial landmark set established in this study reduces data dimensionality and provides a standardized reference framework for future morphometric investigations. Adopting these landmarks as standards by researchers studying skulls of the same species ensures data compatibility, enabling direct comparisons across independent studies. This standardized set facilitates the integration of data from diverse research groups or temporal periods for shape variation assessments and discriminant analyses, including Canonical Variate Analysis (CVA) and Discriminant Function Analysis (DFA).

In developing the reference landmark set, points were positioned on distinct, easily identifiable anatomical structures to ensure repeatability and inter-study compatibility. Bony prominences and cranial suture lines were prioritized as landmark locations due to their consistent identifiability. Dental structures were excluded as landmarks, as teeth may be damaged, worn, or absent in many specimens, rendering them unreliable for standardized reference. This approach enhances data consistency across studies, minimizes observer-related variation, thereby improving the overall reliability and reproducibility of the morphometric dataset.

To mitigate preparation-induced artifacts, the rostral tips of the left and right nasal bones were not designated as separate landmarks; instead, a single mid-point landmark was placed between them. This approach accounts for potential lateral displacement of nasal bones during skull preparation, particularly following soft tissue removal through boiling, which may not reflect *in vivo* morphology. By consolidating these landmarks, the reference set minimizes artificial variation, enhancing the reliability and reproducibility of morphometric data.

To further promote data interoperability, researchers are encouraged to provide landmark coordinate data as supplementary material. This practice enhances transparency, facilitates data reuse, and enables direct comparisons across studies. While sharing complete 3D skull models is an alternative, their large file sizes pose challenges for storage, transfer, and processing. Consequently, sharing landmark coordinate data in standardized formats (e.g., STL, PLY, or OBJ) is preferred, as it simplifies storage and analysis while preserving essential morphometric information. The integration of a standardized landmark scheme with shared coordinate data significantly improves the comparability, reusability, and long-term utility of morphometric datasets.

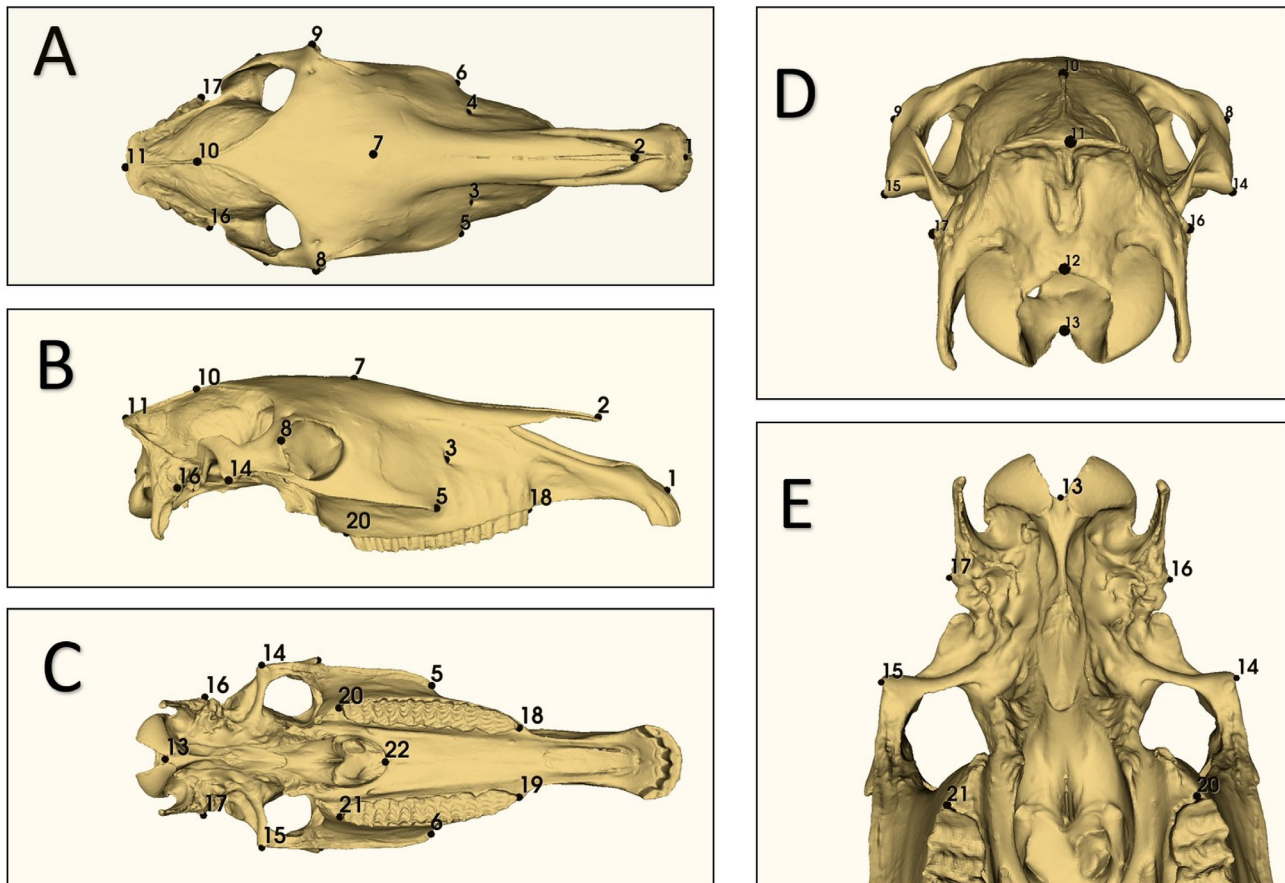


Fig. 1. Reference landmark configuration for the horse skull.

Table 1. Anatomical description of the skull landmarks for the horse used in this study.

Landmark No.	Description
1	Median point of the line joining the most rostral points of the incisive bone (Prosthion)
2	Median point of the line joining the most rostral points of the nasal bones (Rhinion)
3-4	Infraorbital foramen
5, 6	Most rostral point of the facial crest
7	Median point of the naso-frontal suture (Nasion)
8, 9	Most lateral point of the frontal bone on the occipital side of the orbit (Ectorbitale)
10	Median point of the parieto-frontal suture (Bregma)
11	Most caudal point of the external sagittal crest
12	Most dorsal point of the foramen magnum in the median plane (Opisthion)
13	Most ventral point of the foramen magnum in the median plane (Basion)
14, 15	Most lateral point of the articular tubercle
16, 17	Most lateral point of the mastoid process (Otion)
18, 19	Most rostral point of the first premolar alveolus
20, 21	Most caudal point of the last molar alveolus
22	Most caudal point of the horizontal part of the bony palate in the median plane (Staphylion)

In establishing the reference landmark set, priority was given to anatomical regions previously identified as significant contributors to interspecific or interbreed variation. The occipital (nuchal) region was empha-

sized due to its pronounced variability across species. Similarly, landmarks were strategically placed to capture transverse cranial breadth and elongated or narrow cranial morphologies, which are critical determinants

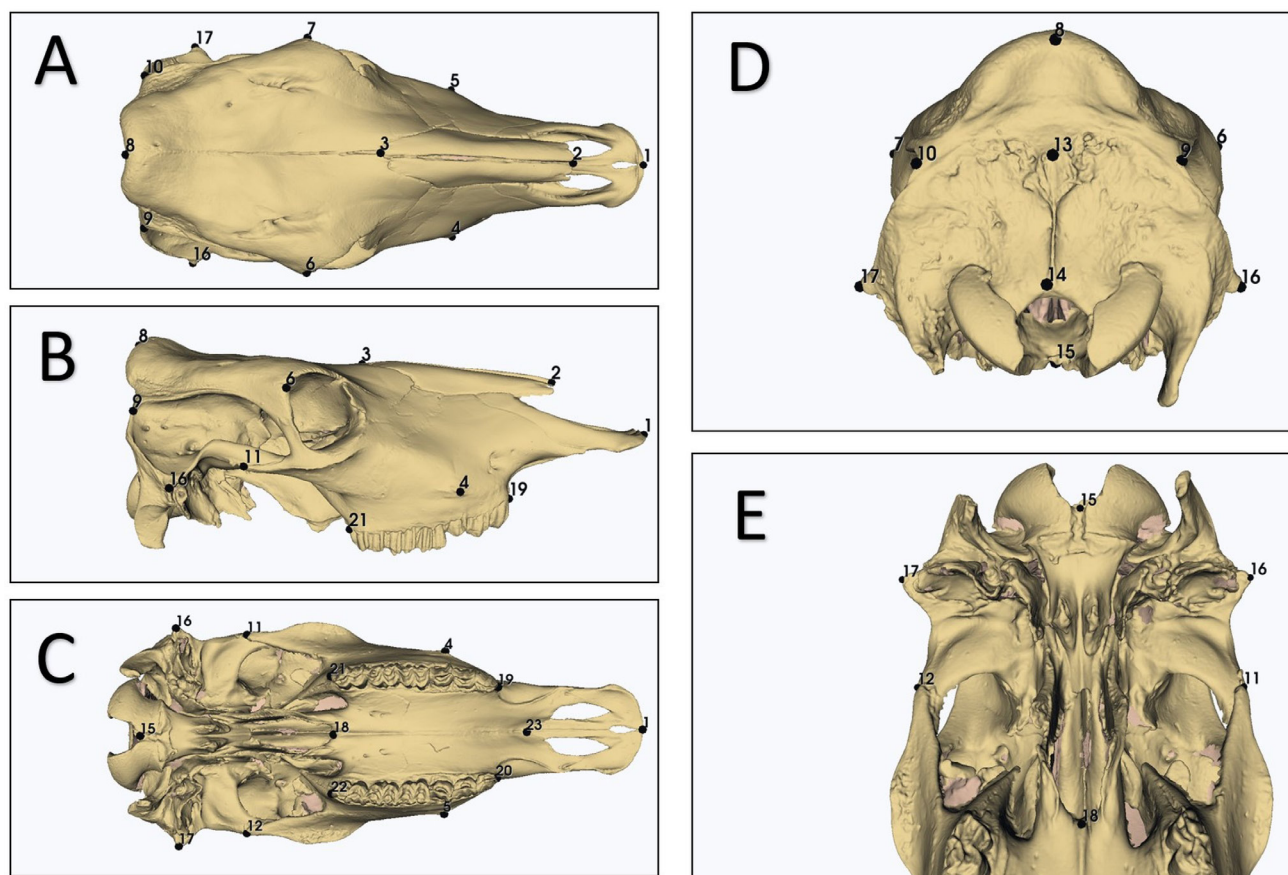


Fig. 2. Reference landmark configuration for the cattle skull.

Table 2. Anatomical description of the skull landmarks for cattle used in this study.

Landmark No.	Description
1	The median point of the line joining the most rostral points of the incisive bone (Prosthion)
2	The median point of the line joining the most rostral points of the nasal bones (Rhinion)
3	The median point of the naso-frontal suture (Nasion)
4, 5	The facial tuber
6, 7	The most lateral point of the frontal bone on the occipital side of the orbit (Ectorbitale)
8	The most caudal point of the vertex of the cranium
9, 10	The most caudal point of the linea temporalis
11, 12	The most lateral point of the articular tubercle
13	The external occipital protuberance
14	The most dorsal point of the foramen magnum
15	The most ventral point of the foramen magnum
16, 17	The external acoustic pore
18	The most caudal point of the horizontal part of the bony palate in the median plane (Staphylion)
19, 20	The most rostral point of the first premolar alveolus
21, 22	The most caudal point of the last molar alveolus
23	The median point of the maxillo-incisive suture

of shape variation. However, certain anatomically significant structures, such as the supraorbital foramen, were excluded due to their minimal contribution to overall cranial shape variation compared to other

regions, including the zygomatic arch, cranial vault, and occipital bone. In contrast, the infraorbital foramen was included for horses, given their elongated facial region relative to other domestic mammals, ensuring

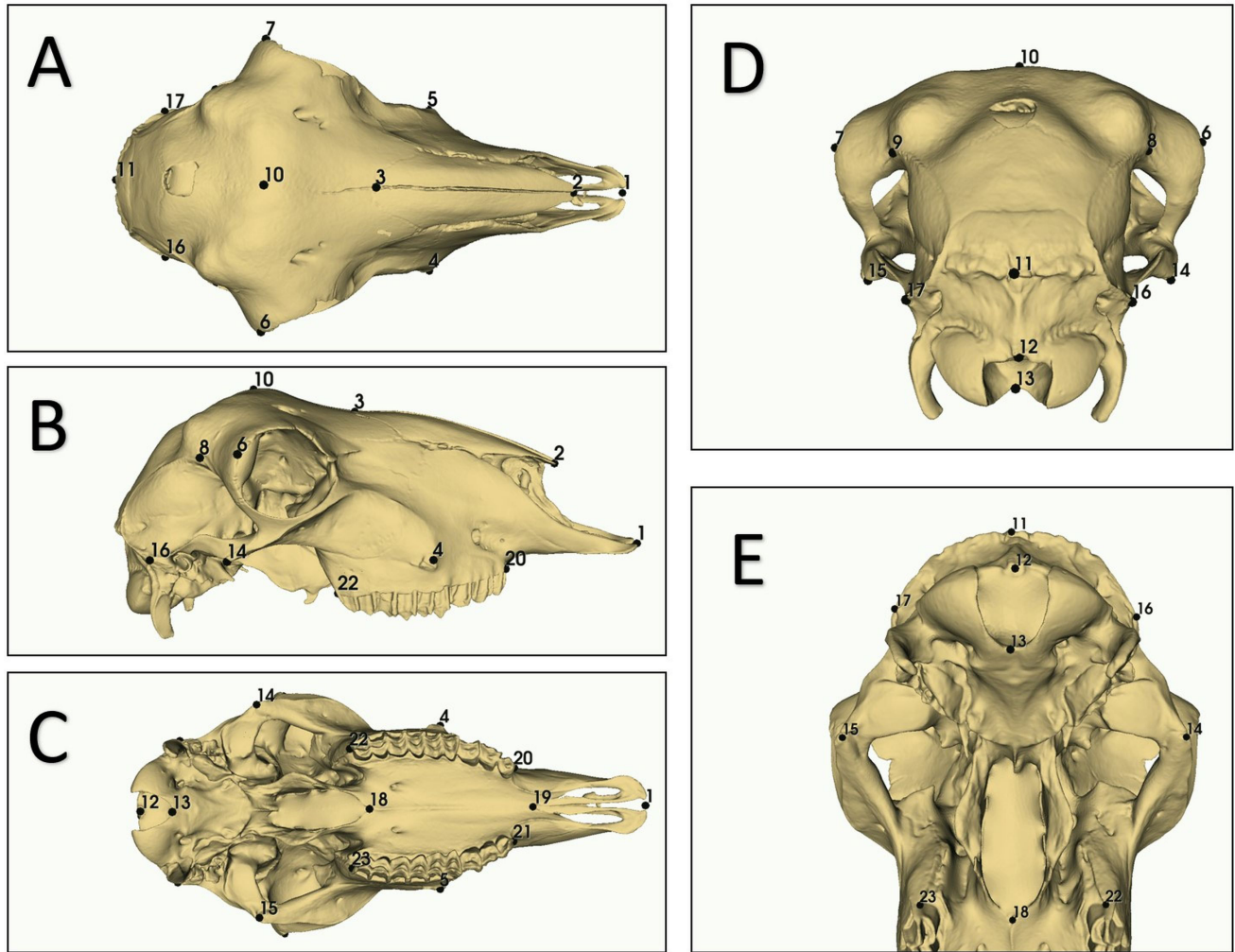


Fig. 3. Reference landmark configuration for the sheep skull.

Table 3. Anatomical description of the skull landmarks for sheep used in this study.

Landmark No.	Description
1	Median point of the line joining the most rostral points of the incisive bone (Prosthion)
2	Median point of the line joining the most rostral points of the nasal bones (Rhinion)
3	Median point of the naso-frontal suture (Nasion)
4, 5	Facial tuber
6, 7	Most lateral point of the frontal bone on the occipital side of the orbit (Ectorbitale)
8, 9	Most rostral point of the temporal line
10	Highest point of the vertex of the cranium
11	External occipital protuberance
12	Most dorsal point of the foramen magnum
13	Most ventral point of the foramen magnum
14, 15	Most lateral point of the articular tubercle
16, 17	Most lateral point of the mastoid process (Otion)
18	Most caudal point of the horizontal part of the bony palate in the median plane (Staphylion)
19	Median point of the maxillo-incisive suture
20, 21	Most rostral point of the first premolar alveolus
22, 23	Most caudal point of the last molar alveolus

a balanced distribution of landmarks and comprehensive capture of equine cranial morphology.

In geometric morphometric analyses, landmarks are evaluated collectively, and the inclusion of numerous low-impact points can unnecessarily increase data dimensionality, reducing statistical power and complicating biological interpretation. An overabundance of low-impact points can diminish the prominence of the primary axes (PCs) that account for significant shape variation. Therefore, the reference landmark set was restricted to key cranial regions: posterior (occipital), anterior (naso-frontal), and lateral (zygomatic arch and orbit), which most effectively reflect morphological differences. This approach ensures the resulting analyses remain biologically meaningful, statistically robust, and readily interpretable.

In addition to manual landmarking, automatic landmarking has emerged as a valuable technique, particularly for skeletal elements with limited or poorly defined anatomical features, such as the calcaneus or talus, where homologous points are difficult to identify (Ünal et al. 2025). By distributing semilandmarks or pseudolandmarks evenly across surfaces, automatic landmarking enables comprehensive shape quantification while minimizing observer bias.

However, this approach presents specific challenges regarding data sharing and reproducibility. Unlike fixed anatomical landmarks, which can be shared as compact coordinate files, automatic landmarks cannot be effectively transferred as standalone coordinates, as their positions depend on the specific alignment and surface-meshing protocols used during processing. To ensure reproducibility, automatic landmarking datasets should be distributed as complete 3D surface models, allowing researchers to reapply the landmarking procedure within the same software environment (e.g., via standardized templates or automated scripts). Sharing only coordinate files would lead to inconsistencies, as the spatial context and meshing parameters required to reproduce the landmark configuration would be lost.

Another critical consideration in automatic landmarking involves the segmentation process of CT-derived models. Following threshold adjustments and segmentation, microscopic residual artifacts, often invisible to the naked eye, can remain around the model. Although these remnants are not part of the anatomical structure, automatic landmarking algorithms may interpret them as part of the model's surface and place landmarks on these regions, introducing artificial variation into the dataset. Such errors typically manifest as abnormal distributions or outliers during PCA, distorting the interpretation of shape variation. Therefore, thorough post-processing and artifact removal are crucial when preparing CT-based 3D models prior to landmarking.

In contrast, models obtained from 3D surface scanners inherently avoid many of these issues, as they capture only the specimen's external surface geometry. Unlike CT-derived models, they are less prone to microartifacts and segmentation-induced irregularities, providing a cleaner, more reliable basis for automatic landmarking.

Data and metadata sharing standard

To align with the FAIR (Findable, Accessible, Interoperable, Reusable) principles in veterinary morphometrics, we recommend sharing 3D models in mesh formats (STL, PLY, OBJ) via repositories such as MorphoSource or Zenodo, accompanied by metadata on acquisition methods, software versions, and segmentation parameters. Landmark coordinates should be provided in tabular formats (CSV, TPS, .fcsv) with details on landmark definitions, observer information, and GPA alignment protocols. This standard facilitates reproducibility and cross-study integration.

Statistical analyses

In three-dimensional geometric morphometric studies, the primary dataset comprises the X, Y, and Z coordinates of landmarks, the Procrustes coordinates derived from Generalized Procrustes Analysis, and the centroid size (CS), which represents the overall size of each specimen (Bookstein 1996, Cooke and Terhune 2015). GPA aligns all specimens within a standard reference frame by eliminating the effects of size (scale), position (translation), and orientation (rotation), preserving only shape-related information. The resulting Procrustes coordinates form the standardized dataset for analyzing shape variation. Centroid size, calculated as the square root of the summed squared distances of all landmarks from their centroid, serves as a metric for overall size (Rohlf 2002, Mitteroecker and Gunz 2009). Together, CS and Procrustes coordinates enable quantification of the extent of shape variation associated with size or growth (allometry). Size-adjusted coordinates can then be used to assess shape differences between groups, independent of size effects.

Principal Component Analysis (PCA) is the primary method for summarizing and visualizing variation in high-dimensional morphometric datasets (Polly et al. 2013, Klingenberg and Marugán-Lobón 2013). PCA identifies principal axes (PCs) that account for the largest proportions of shape variation, thereby reducing dimensionality. PCs should be selected and interpreted based on scree plots and biological relevance, focusing on those explaining substantial proportions of variance

rather than adhering to a fixed threshold. Typically, the first few PCs (e.g., PC1 and PC2) capture most of the total variation, facilitating visualization and interpretation. Only PCs explaining $\geq 10\%$ of total variation are generally reported, as those contributing minimal proportions (e.g., $< 5\%$) offer limited biological insight (Rummel et al. 2024). PCA is a fundamental tool for exploring the distribution and overlap of shape variation among different species, breeds, sexes, or age groups.

To enhance group separation, PCA is often complemented by Canonical Variate Analysis (CVA) and Discriminant Function Analysis (DFA) (Lawing and Polly 2010, Manthey and Ousley 2020). CVA projects data into a multivariate space that minimizes within-group variation while maximizing between-group variation, generating axes that optimally highlight morphological differentiation among groups. When paired with CVA, DFA evaluates the classification accuracy of specimens into their respective groups, quantifying the efficacy of shape-based discrimination.

Procrustes ANOVA is employed to assess the statistical significance of shape differences among groups (e.g., species, sexes), while controlling for observer or technical errors, thus determining the extent to which variation identified by PCA and CVA is attributable to group identity (Klingenberg and McIntyre 1998). To validate landmark repeatability, a Procrustes ANOVA with “observer” as a factor is recommended, along with simulations to evaluate the effects of landmark reduction on PCA stability. Complementary techniques, such as PERMANOVA for testing shape distances, and analyses of modularity and integration, can situate the work within broader methodological standards. Allometric analysis, typically conducted through multivariate regression of Procrustes coordinates against CS, examines the relationship between shape and size (Mitteroecker et al., 2013; Klingenberg 2016). This approach quantifies the proportion of shape variation driven by growth or size differences versus by intrinsic morphological traits, enabling size-corrected intergroup comparisons that focus on shape-driven variation.

Landmark coordinates are typically acquired using software tools such as Stratovan Checkpoint, MorphoJ, or 3D Slicer and then exported for further statistical analysis (Klingenberg 2011, Rolfe et al. 2021, Boz et al. 2023). These datasets are processed in statistical environments such as SPSS or R, where morphometric analyses, including PCA, Procrustes ANOVA, and regression, are performed. To ensure compatibility and interoperability across platforms, only standardized Procrustes coordinates following GPA, rather than raw 3D models, should be used for these analyses.

This practice enhances data sharing and reproducibility across studies.

Applications and future perspectives of 3D morphometrics

Three-dimensional (3D) geometric morphometrics has become an increasingly important methodology across disciplines, including veterinary anatomy, taxonomy, evolutionary biology, and animal breeding. This approach offers significant advantages for precise modeling and comparison of skeletal structures, the identification of morphological differences at the species and breed levels, and the exploration of functional-anatomical relationships. Moreover, 3D morphometrics provides a sustainable research framework by generating archivable, reanalyzable digital datasets that overcome the limitations of traditional linear and angular morphometric measurements.

In veterinary applications, 3D morphometrics facilitates species and breed identification, assessment of morphologies associated with performance and health traits in livestock, and classification of fossil and archaeological specimens. In clinical contexts, 3D morphometric data support orthopedic surgical planning, biomechanical modeling, and the evaluation of congenital anomalies, enabling enhanced diagnostic precision and more effective therapeutic interventions.

Advancements in 3D morphometric technology are anticipated to drive the adoption of automated landmarking and artificial intelligence (AI)-driven analyses. Deep learning algorithms, in particular, offer the potential for faster and more consistent landmark detection and shape classification compared to manual methods. Furthermore, integrating augmented reality (AR) and virtual reality (VR) applications is expected to enhance veterinary education and research, enabling the interactive use of morphometric models and introducing a new dimension to learning and training.

Despite its potential, the widespread adoption of 3D morphometrics presents challenges, particularly in data standardization and sharing. Establishing international databases and standardized reference landmark sets will be essential to ensure study comparability. Such initiatives will enable large-scale datasets to yield novel insights into morphological diversity, adaptation, and health-related variation.

In conclusion, 3D geometric morphometrics remains a cornerstone analytical tool in veterinary anatomy and morphology, with its significance amplified by its integration with AI, AR, VR, and large-scale data-driven research frameworks.

Authors declarations

Ethics approval

Ethical approval was not required for this study. This work is a review article that summarizes previously published research. No new experimental procedures involving live animals were conducted, and no primary data collection from live subjects occurred.

Use of generative artificial intelligence

No generative artificial intelligence (AI) tools were used in the preparation of this manuscript. All content was produced by the authors.

Conflict of interest

The authors declare no conflicts of interest.

References

- Ahmed A, Hamam O, Niri SG, Oeltzchner G, Garg T, Elmandouh O, Intrapromku J, Yedavalli V (2023) Computed tomography perfusion stroke mimics on RAPID commercial software: A case-based review. *Brain Circ* 9: 68-76.
- Atli MZ, İşbilir F, Güzel BC (2025) Siirt-colored mohair goat (*Capra hircus*) and Romanov Sheep (*Ovis aries*) Determination of Morphometric Features of Hyoid Bone via Three Dimensional Modelling. *Dicle Univ Vet Fak Derg* 18: 19-22.
- Bakici C, Kilicli IB, Yunus HA, Ünal İ, Batur, B (2025) Evaluating sexual dimorphism in Romanov sheep: A comparative 3D shape analysis of manual and automated landmarking. *Ann Anat*, 262, 152708.
- Bjørndal L, Carlsen O, Thuesen G, Darvann T, Kreiborg S (1999) External and internal macromorphology in 3D-reconstructed maxillary molars using computerized X-ray microtomography. *Int Endod J* 32: 3-9.
- Bookstein FL (1996) Combining the tools of geometric morphometrics. In *Advances in morphometrics*. Boston, MA: Springer US, pp. 131-151.
- Bookstein FL (1997) *Morphometric tools for landmark data*. Cambridge, UK: Cambridge University Press, pp. 455.
- Boz I, Manuta N, Özkan E, Kahvecioğlu O, Pazvant G, Gezer Ince N, Hadžiomerović N, Szara T, Altundağ Y, Gündemir O (2023) Geometric morphometry in veterinary anatomy. *Veterinaria* 72: 15-27.
- Carballido-Gamio J, Link TM, Li X, Han ET, Krug R, Ries MD, Majumdar S (2008) Feasibility and reproducibility of relaxometry, morphometric, and geometrical measurements of the hip joint with magnetic resonance imaging at 3T. *J Magn Reson Imaging* 28: 227-235.
- Cardini A, Elton S (2007) Sample size and sampling error in geometric morphometric studies of size and shape. *Zoomorphology* 126: 121-134.
- Cardini A, Seetah K, Barker G (2015) How many specimens do I need? Sampling error in geometric morphometrics: testing the sensitivity of means and variances in simple randomized selection experiments. *Zoomorphology* 134: 149-163.
- Cooke SB, Terhune CE (2015) Form, function, and geometric morphometrics. *Anat Rec* 298: 5-28.
- Fedorov A, Beichel R, Kalpathy-Cramer J, Finet J, Fillion-Robin JC, Pujol S, Bauer C, Jennings D, Fennessy F, Sonka M, Buatti J, Aylward S, Miller JV, Pieper S, Kikinis R (2012) 3D Slicer as an image computing platform for the Quantitative Imaging Network. *Magn Reson Imaging* 30: 1323-1341.
- Hadžiomerović N, Gundemir O, Tandir F, Avdić R, Katica M (2023) Geometric and morphometric analysis of the auditory ossicles in the red fox (*Vulpes vulpes*). *Animals* 13: 1230.
- Han J, Wu M, Ge Y (2019) A study on the dimension accuracy on the inner structure of the 3D printed parts caused by the scanning strategy. *Materials* 12: 1333.
- Haruda A F, Varfolomeev V, Goriachev A, Yermolayeva A, Outram AK (2019) A new zooarchaeological application for geometric morphometric methods: distinguishing *Ovis aries* morphotypes to address connectivity and mobility of prehistoric Central Asian pastoralists. *J Archaeol Sci*, 107, 50-57.
- Haverkamp K, Harder LK, Kuhnt NSM, Lüpke M, Nolte I, Wefstaedt P (2019) Validation of canine prostate volumetric measurements in computed tomography determined by the slice addition technique using the Amira program. *BMC Vet Res* 15: 49.
- Hennessy RJ, McLearn S, Kinsella A, Waddington JL (2005) Facial surface analysis by 3D laser scanning and geometric morphometrics in relation to sexual dimorphism in cerebral – craniofacial morphogenesis and cognitive function. *J Anat* 207: 283-295.
- Herzlinger G, Goren-Inbar N, Grosman L (2017) A new method for 3D geometric morphometric shape analysis: The case study of handaxe knapping skill. *J Archaeol Sci Rep* 14: 163-173.
- Hirst CS, White S, Smith SE (2018) Standardisation in 3D geometric morphometrics: Ethics, ownership, and methods. *Archaeologies* 14: 272-298.
- İşbilir F, Güzel BC (2023) Determination of Morphometric Characteristics of Glandula Lacrimalis in Siirt-Colored Mohair Goat (*Capra hircus*) and Romanov Sheep (*Ovis aries*) by Computed Tomography Images. *Dicle Univ Veter Fak Derg*, 16: 96-101.
- Klingenberg CP (2011) MorphoJ: an integrated software package for geometric morphometrics. *Mol Ecol Resour* 11: 353-357.
- Klingenberg CP (2016) Size, shape, and form: concepts of allometry in geometric morphometrics. *Dev Genes Evol* 226: 113-137.
- Klingenberg CP, Marugán-Lobón J (2013) Evolutionary covariation in geometric morphometric data: analyzing integration, modularity, and allometry in a phylogenetic context. *Syst Biol*, 62: 591-610.
- Klingenberg CP, McIntyre GS (1998) Geometric morphometrics of developmental instability: analyzing patterns of fluctuating asymmetry with Procrustes methods. *Evolution*, 52: 1363-1375.
- Korkmazcan A, Ünal B, Bakıcı C, Gündemir O (2025) Exploring skull shape variation and allometry across different chicken breeds. *Ankara Univ Vet Fak Derg* 72: 1-7.

- Lawing AM, Polly PD (2010) Geometric morphometrics: recent applications to the study of evolution and development. *J Zool* 280: 1-7.
- Manthey L, Ousley SD (2020) Geometric morphometrics. In: Obertova Z, Stewart A, Cattaneo C (eds) *Statistics and probability in forensic anthropology*. Academic Press, London, pp. 289-298.
- Manuta N, Çakar B, Gündemir O, Spataru MC (2024) Shape and size variations of distal phalanges in cattle. *Animals* 14: 194.
- Mitteroecker P, Gunz P (2009) Advances in geometric morphometrics. *Evol Biol* 36: 235-247.
- Mitteroecker P, Gunz P, Windhager S, Schaefer K (2013) A brief review of shape, form, and allometry in geometric morphometrics, with applications to human facial morphology. *Hystrix* 24: 59-66.
- Pasicka E, Janeczek M, Gündemir O (2025) Skull morphology of shepherd dogs in Poland. *Ankara Üniv Vet Fak Derg* 72(3), 305-312.
- Percie du Sert N, Hurst V, Ahluwalia A, Alam S, Avey MT, Baker M, Browne WJ, Clark A, Cuthill IC, Dirnagl U, Emerson M, Garner P, Holgate ST, Howells DW, Karp NA, Lazić SE, Lidster K, MacCallum CJ, Macleod M, Pearl EJ, Petersen OH, Rawle F, Reynolds P, Rooney K, Sena ES, Silberberg SD, Steckler T, Würbel H (2020) The ARRIVE guidelines 2.0: Updated guidelines for reporting animal research. *Journal of Cerebral Blood Flow & Metabolism*, 40(9), 1769-1777.
- Polly PD, Lawing AM, Fabre AC, Goswami A (2013) Phylogenetic principal components analysis and geometric morphometrics. *Hystrix*, 24: 33-41.
- Rohlf FJ (2002) Geometric morphometrics and phylogeny. *Systematics Association Special Volume*, 64: 175-193.
- Rolfe S, Pieper S, Porto A, Diamond K, Winchester J, Shan S, Kirveslahti H, Boyer D, Summers A, Maga AM (2021) SlicerMorph: An open and extensible platform to retrieve, visualize and analyse 3D morphology. *Methods Ecol Evol* 12: 1816-1825.
- Rummel AD, Sheehy ET, Schachner ER, Hedrick BP (2024) Sample size and geometric morphometrics methodology impact the evaluation of morphological variation. *Integr Org Biol* 6: obae002.
- Sood A, Dogra V, Pathmanathan G (2021) 3D surface digitization in scientific research and product development. *Forensic Med Anat Res* 9: 11-23.
- Thali MJ, Braun M, Dirnhofer R (2003) Optical 3D surface digitizing in forensic medicine: 3D documentation of skin and bone injuries. *Forensic Sci Int* 137: 203-208.
- Tretiakow D, Tesch K, Meyer-Szary J, Markiet K, Skorek A (2021) Three-dimensional modeling and automatic analysis of the human nasal cavity and paranasal sinuses using the computational fluid dynamics method. *Eur Arch Otorhinolaryngol* 278: 1443-1453.
- Ünal B, Güzel BC, Çakar B, Kanmaz YA, Yiğit F, Gündemir O, Spataru MC (2025) Shape and Size Variations in the Astragalus of Large and Small Bovids. *Animals* 15: 425.
- Van der Niet T, Zollikofer CP, de León MSP, Johnson SD, Linder HP (2010). Three-dimensional geometric morphometrics for studying floral shape variation. *Trends Plant Sci* 15: 423-426.
- Zelditch M, Swiderski D, Sheets HD (2012) *Geometric Morphometrics for Biologists: A Primer*. Elsevier. Amsterdam.